Crystal Conformation of the Cyclic Decapeptide Phakellistatin 8: Comparison with Antamanide

Delbert L. Herald,[†] Giovanni L. Cascarano,[‡] George R. Pettit,*[,†] and Jayaram K. Srirangam[†]

Contribution from the Cancer Research Institute and Department of Chemistry, Arizona State University, Tempe, Arizona 85287-2404, and CNR-IRMEC c/O Dipartimento Geomineralogico, Campus Universitario, 70125 Bari, Italy

Received July 31, 1996[⊗]

Abstract: The solid-state conformation of the cyclic decapeptide phakellistatin 8, cyclo[Pro_1-Pro_2-Ile_3-Phe_4-Val_5-Leu_6-Pro_7-Pro_8-Tyr_9-Ile_{10}] has been determined by X-ray methods. [Crystal data: orthorhombic; $P2_12_12$; a = 20.294(2), b = 24.141(6), c = 13.903(3) Å. Least-squares refinement of 10061 reflections ($I > 2\sigma(I)$) led to residuals $R_1 = 0.0651$ (Sheldrick $wR_2 = 0.1749$).] The cyclic decapeptide includes (1) a 5→1 transannular α-turn type H-bond, encompassing the Pro_1, Pro_2, and Ile_3 residues and involving the Phe_4 amide hydrogen and the Ile_{10} carbonyl, (2) an intramolecular 3→1 type VIa γ-turn type of H-bond, encompassing the Phe_4 residue and involving the Val_5 amide hydrogen and the Ile_3 carbonyl, and (3) an intramolecular 4→1 type VIa β-turn H-bond, encompassing the Pro_7 and Pro_8 residues and involving the Tyr_9 amide hydrogen and the Leu_6 carbonyl. All backbone dihedral angles fall within normal, low-energy regions except for two amino acid residues, Phe_4 (Φ, Ψ = 71°, −41°) and Tyr_9 (Φ, Ψ = 75°, 31°), the side chains of which are found to fold back over the peptide backbone. Conformations of the four proline residues for phakellistatin 8 can be classified as follows: Pro_1 C_s-C$^\gamma$*exo*, Pro_2 C_2-C$^\beta$*exo*(C$^\gamma$*endo*), Pro_7 C_s-C$^\gamma$endo and Pro_8 C_2-C$^\beta$exo(C$^\gamma$endo). Examination of phakellistatin 8 and the decapeptide antamanide show the two compounds are quite similar, both in overall backbone conformation, proline ring conformations, and the presence of nearly identical α-turns involving one of the Pro-Pro pairs. Both molecules are highly hydrated when crystallized from aqueous solvents and both exhibit channel formation in the solid state.

1. Introduction

An increasing number of cyclic peptides, from both synthetic and natural origin, are being reported each year. A majority of these peptides are of the smaller ring variety (i.e., cyclic penta-, hexa-, hepta-, and octapeptides). Fewer larger ring peptides have been reported, particularly those isolated from natural sources and exhibiting biological activity. In the latter group are the cyclic decapeptides, several of which have been the subjects of extensive examination and reviews and have played an important role in the history of peptide conformational analysis. These are, in order of increasing number of literature citations: the tyrocidines,[1] the structurally related gramicidin S,[1,2] and antamanide (**1**) and its analogs.[3] The first two decapeptides have received considerable attention, primarily due to the varying degrees of antibiotic activity exhibited by these compounds toward bacteria.[4] Both gramicidin S and the tyrocidines are known to damage the cytoplasmic membranes of sensitive microorganisms and to release nucleotides from the cytoplasm. In the case of gramicidin S, it has been speculated that its biological activity may be due to the ability of the molecules to associate and form large channels.[5] Such channels could then allow ions and particles of a rather large size to pass through in an ion transmembrane transfer process. The third decapeptide, antamanide (name derived from the term anti-amanita peptide, **1**), isolated from the extracts of the poisonous mushroom *Amanita phalloides* (also known as the green death cup) has probably received even greater attention. Indeed, it appears to be one of the most extensively examined cyclic peptides to date.

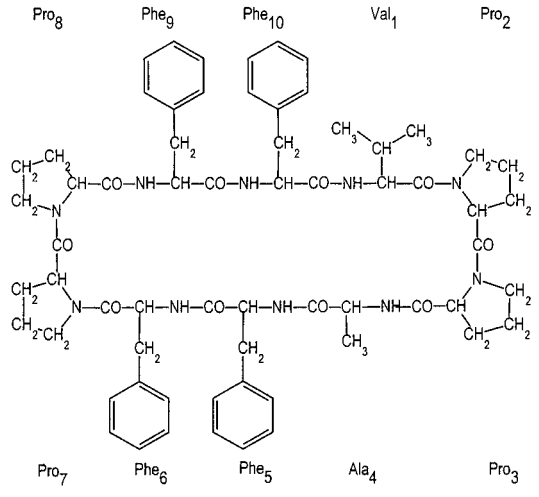

1

Interest in antamanide was presumably initially inspired by the observation that preadministration of this peptide to labora-

[†] Arizona State University.
[‡] Campus Universitario.
[⊗] Abstract published in *Advance ACS Abstracts,* June 15, 1997.

(1) Izumiya, N.; Kato, T.; Aoyagi, H.; Waki, M. Kondo, M. In *Synthetic Aspects of Biologically Active Cyclic Peptides-Gramicidin S and Tyrocidines*; Kodansha Ltd.: Tokyo 1979, and references therein.

(2) (a) Dygert, M.; Gō, N.; Scheraga, H. *Macromolecules* **1975**, *8*, 750−61. (b) Rackovsky, S.; Scheraga, H. *Proc. Natl. Acad. Sci. U.S.A.* **1980**, *77* (12), 6965−7. (c) Harding, M. In *Structural Studies on Molecules of Biological Interest, A Volume in Honour of Professor Dorothy Hodgkin*; Dodson, G., Glusker, J., Sayre, D., Eds.: Oxford University Press: New York, NY, 1981; pp 199−206. (d) Nemethy, G.; Scheraga, H. *Biochem. Biophys. Res. Commun.* **1984**, *118* (2), 643−7. (e) Liquori, A.; De Santis, P. *Int. J. Biol. Macromol.* **1980**, *2* (2), 112−15.

(3) Wieland, T. In *Peptides of Poisonous Amanita Mushrooms*; Rich, A., Ed.; Springer Series in Molecular Biology. Springer-Verlag: New York, NY, 1986; pp 181−247. A more complete listing of references concerning the tyrocidines, gramicidin S and antamanide is included in the Supporting Information.

(4) Hotchkiss, R. In *Lauching the Antibiotic Era*; Moberg, C., Cohn, Z., Eds.; The Rockefeller University Press: New York, NY 1990.

S0002-7863(96)02664-9 CCC: $14.00

tory animals provided prophylactic protection from the lethal affects of the phallotoxins present in the same mushroom.[3] More recently, antamanide has been reported to exhibit immunosuppresive activity,[6] thus presumably providing additional motivation. After its initial isolation, a number of rather unique structural features were found to be exhibited by antamanide and its derivatives from both X-ray[7] and NMR[8] experiments. These preliminary experiments have fostered an ongoing series of investigations, primarily directed at determining the mechanism of action in biological systems and ascertaining its bioactive, solution conformation(s).[5b,11b] In general, to determine such peptide solution conformations, molecular modeling[9] and energy minimization procedures[10] are often used to examine energetically favorable conformations. A prerequisite of such procedures is that an accurate, three-dimensional description of the molecule be available before sensible experiments can be conducted. As a result, molecular modeling and conformer energy minimization investigations have relied extensively upon the results of previous X-ray crystallographic experiments. These experiments provide not only an accurate description of the atomic connectivity of molecules, but also a wealth of additional information such as bond lengths, bond angles, inter- and intramolecular interactions, solid-state conformational details, along with molecular packing and hydrogen bonding. This information, coupled with NMR observations obtained from solution (NOE effects, chemical shifts, coupling constants, and relaxation times) has proven to be a most effective technique for the successful refinement of the multitude of possible conformations leading to the presumably "biologically active" low-energy, solution conformer(s).[11] Consequently, the use of crystal coordinates has served as a logical departure point for a majority of modeling and energy-minimization experiments. In the case of the cyclic peptides, this method should be expected to be particularly effective in determining the geometry of the solution conformer owing to the inherent constraints placed upon the possible conformational models by the presence of the ring itself.

Recently, we reported[12] the isolation of three, new cyclic decapeptides (phakellistatins 7, 8, and 9) from the marine sponge *Phakellia costata*. Because these compounds exhibited cancer cell growth inhibitory properties, we were interested in determining their structures, absolute stereochemistry, and conformational properties. Because the three peptides were quite closely related, it was theorized that the structure determination of any one might well assist in elucidating the structures of the other two. Since these cyclic peptides could be obtained in a crystalline state via slow evaporation of saturated solutions of the compounds from polar organic solvents, X-ray crystallographic structure determination was investigated. Not only could the three-dimensional nature of the peptides be established in an unambiguous manner by X-ray, but the additional information regarding crystal conformation, H-bonding, and crystal packing could be utilized in subsequent molecular modeling-energy minimization studies. Of the three peptides, phakellistatin 8 (**2**) seemed to be the best candidate

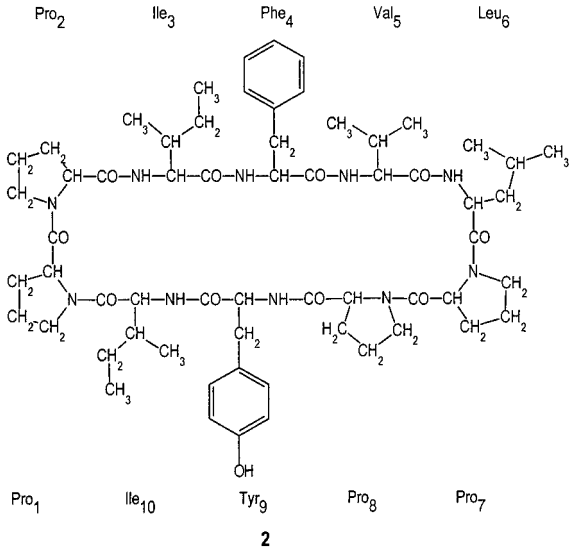

2

for X-ray analysis. Phakellistatin 8 was present in the largest quantity and crystals could be grown from a saturated, aqueous

(5) (a) Tishchenko, G.; Andrianov, V.; Vainshtein, B.; Dodson, E. *Bioorg. Khim.* **1992**, *18* (3), 357−73. (b) Ivanov, V. In *Peptides, Proceedings of the Fifth American Peptide Symposium*; Goodman, M., Meienhofer, J., Eds.; John Wiley & Sons: New York, NY, 1977; pp 307−21.

(6) Siemion, I.; Pedyczak, A.; Trojnar, J.; Zimecki, M.; Wieczorek, Z. *Peptides* **1992**, *13* (6), 1233−7.

(7) (a) Littke, W. *Tetrahedron Lett.* **1971**, *45*, 4247−50. (b) Karle, I.; Karle, J.; Wieland, T.; Burgermeister, W.; Faulstich, H.; Witkop, B. *Proc. Natl. Acad. Sci. U.S.A.* **1973**, *70* (6), 1836−40. (c) Karle, I. *Biochemistry* **1974**, *13* (10), 2155−62. (d) Karle, I.; Karle, J.; Wieland, T.; Burgermeister, W.; Witkop, B. *Proc. Natl. Acad. Sci. U.S.A.* **1976**, *73* (6), 1782−5. (e) Karle, I. *J. Am. Chem. Soc.* **1977**, *99* (15), 5152−57. (f) Karle, I.; Duesler, E. *Proc. Natl. Acad. Sci, U.S.A.* **1977**, *74* (7), 2602−06. (g) Karle, I. *Peptides, Proceedings of the Fifth American Symposium*; Goodman, M.; Meienhofer, J., Eds.; John Wiley & Son: New York, NY, 1977; pp 583−85. (h) Karle, I., *Pept. Struct. Biol. Funct., Proc. Am. Pept. Symp., 6th*; Gross, E., Meienhofer, J., Eds.; Pierce Chem. Co.: Rockford, IL, 1979; pp 681−90. (i) Karle, I.; Wieland, T.; Schermer, D.; Ottenheym, H., *Proc. Natl. Acad. Sci. U.S.A.* **1979**, *76* (4) 1532−36 and references therin. (j) Karle, I. In *The Peptides: Analysis, Synthesis, Biology*; Gross, E., Meienhofer, J. Eds.; Academic Press: New York, NY, 1981; pp 1−53. (l) Karle, I. *Int. J. Pept. Protein Res.* **1986**, *28*, 6.

(8) (a) Patel, D. *Biochemistry* **1973**, *12* (4), 667−676. (b) Burgermeister, W.; Wieland, T.; Winkler, R. *Eur. J. Biochem.* **1974**, *44*, 305−316. (c) Kessler, H; Müller, A.; Oschkinat, H. *Magn. Res. Chem.* **1985**, *23* (10), 844−52. (d) Kessler, H.; Griesinger, J.; Lautz, J.; Müller, A. van Gunsteren, W.; Berendsen, J. C. *J. Am. Chem. Soc.* **1988**, *110*, 3393−6. (e) Kessler, H.; Müller, A.; Pook, K-H. *Liebigs Ann. Chem.* **1989**, *9*, 903−12. (f) Kessler, H.; Bats, J.; Lautz, J.; Müller, A. *Liebigs Ann. Chem.* **1989**, *9*, 913−28. (g) Mádi, Z.; Griesinger, C.; Ernst, R. *J. Am. Chem. Soc.* **1990**, *112* (8), 2908−14. (h) Brüschweiler, R.; Roux, B.; Blackledge, M.; Griesinger, C.; Karplus, M.; Ernst, R. *J. Am. Chem. Soc.* **1992**, *114* (7), 2289−93. (i) Brunne, R.; Van Gunsteren, W.; Brüschweiler, R.; Ernst, R. *J. Am. Chem. Soc.* **1993**, *115* (12), 4764−8. (j) Ernst, R. *Pure Appl. Chem.* **1994**, *66* (8), 1583−8. (k) Ernst, R. *Pure Appl. Chem.* **1994**, *66* (10/11), 1955−60. (l) Bremi, T.; Ernst, M.; Ernst, R. *J. Phys. Chem.* **1994**, *98* (7), 9322−34.

(9) (a) Blundell, T.; Davies, E.; Gasteiger, J.; Glen, R.; Goodford, P.; Hubbard, R.; Langridge, R.; Marshall, G.; Murray-Rust, P; Pearlstein, R.; Quarendon, P.; Richards, W.; White, D. *The Molecular Graphics Society, Computer-Aided Molecular Design*; Oyez Scientific & Technical Services Ltd.: London, 1984. (b) *Crystallographic and Modeling Methods in Molecular Design*; Bugg, C., Ealick, S., Eds.; Springer-Verlag: New York, NY, 1990. (c) Goodfellow, J.; Moss, D. *Computer Modeling of Biomolecular Processes*; Ellis Horwood: New York, NY, 1992.

(10) (a) Levitt, M. *J. Mol. Biol.* **1974**, *82*, 393−420. (b) Zimmerman, S.; Scheraga, H. *Biopolymers* **1977**; *16*, 811−843. (c) Hagler, A. *Theoretical Simulation of Conformation*, Energetics, and Dynamics of Peptides. In *The Peptides*; Academic Press: New York, NY, 1985; pp 213−299. (d) Kitson, D.; Hagler, A. *Biochemistry* **1988**, *27*, 5246−5257. (e) Lautz, J.; Kessler, H.; Blaney, J.; Scheek, R.; Van Gunsteren, W. *Int. J. Peptide Protein Res.* **1989**, *33*, 281−288. (f) Van Gunsteren, W.; Berendsen, H. *Angew. Chem. Int. Ed. Engl.* **1990**, *29*, 992−1023. (g) Daggett, V.; Kollman, P.; Kuntz, I. *Biopolymers* **1991**, *31*, 285−304. (h) Rizo, J.; Koerber, S.; Bienstock, R.; Rivier, J.; Gierasch, L.; Hagler, A. *J. Am. Chem. Soc.* **1992**, *114*, 2860−71. (i) McDowell, R.; Gadek, T.; Barker, P.; Burdick, D.; Chan, K.; Quan, C.; Skelton, N.; Struble, M.; Thorsett, E.; Tischler, M.; Tom, J.; Webb, T.; Burnier, J. *J. Am. Chem. Soc.* **1994**, *116*, 5069−76.

(11) For reviews on the application of NMR and other physical data in conformational analyses, see: (a) Smith, J.; Pease, L. *CRC Crit. Rev. Biochem.* **1980**, *8* (4), 315−99. (b) Rose, G.; Gierasch, L.; Smith, J. *Adv. Protein Chem* **1980**, *37*, 1−109. (c) Konant, R.; Mierke, D.; Kessler, H.; Kutscher, B.; Bernd, M.; Voegeli, R. *Helv. Chim. Acta* **1993**, *76*, 1649−66. (d) Eggleston, D.; Baures, P.; Peishoff, C.; Kopple, K. *J. Am. Chem. Soc.* **1991**, *113*, 4410−16. (e) Peishoff, C.; Bean, J.; Kopple, K. *J. Am. Chem. Soc.* **1991**, *113*, 4416−21.

(12) Pettit, G.; Xu, J-P; Dorsaz, A-C.; Williams, M.; Boyd, M.; Cerny, R. *Bioorg. Med. Chem. Lett.* **1995**, *5* (13), 1339−44.

methanol solution. Consequently, several separate X-ray data collections were conducted on this compound. Unfortunately, X-ray structure solution of phakellistatin 8 proved to be extremely difficult, and NMR techniques were eventually resorted to in order to assign structures to each of the three cyclic peptides. A description of the isolation and NMR structure determination of these compounds has been reported elsewhere.[12] A solution to the X-ray structure problem of phakellistatin 8 remained unsolved until recently, when that obstacle was finally overcome via application of a new direct methods solution program to the problem. We now report the X-ray structure solution for phakellistatin 8 (**2**) and an analysis of the solid-state conformation assumed by this peptide. Because of a number of structural similarities (i.e., presence of two cis Pro−Pro peptide units, extensive hydrogen bonding, and overall solid-state conformational aspects), some comparisons between phakellistatin 8 (**2**) and antamanide (**1**) were also studied.

2. Methods

Initial experimental data (NMR and mass spectroscopy) indicated that all three phakellistatins were composed completely of the common amino acids, thus signifying the compounds were true peptides. Mass spectral data also suggested the three peptides were closely related, as well as being cyclic. The amino acid units for phakellistatin 8 (**2**) were determined to be Pro, Ile, Leu, Val, Phe, and Tyr in the ratio of 4:2:1:1:1:1. This implied a molecular formula weight of 1137. Space group determination ($P2_12_12$) coupled with density measurements of phakellistatin 8 disclosed that the unit cell contained four molecules of the parent peptide, as well as the presence of additional solvent molecules, the MW for the asymmetric unit being 1230.

Four different data collections were conducted on phakellistatin 8. The initial X-ray data collection was performed at ambient temperature (298 K) with Cu radiation, in which Friedel reflections were collected along with the unique octant of reflections. Subsequent, concerted attempts at direct method solutions were undertaken using the programs MULTAN,[13a] RANTAN,[13b] MAGIC and YZARC,[13c] MAGEX,[13d] MITHRIL,[14] SHELXS-86,[15] SIMPEL,[16] SIR88,[17] and SIR92.[18] In each case, although structural fragments could often be obtained, no chemically sensible chain of atoms could be found which could be identified as part of a peptide sequence. The vector search program PATSEE[19] also failed to locate any proline fragments when that amino acid moiety was used as the search input fragment.

Because all direct methods solution attempts had failed on the first collection, additional data collections were undertaken. Since the success or failure of direct methods programs can often be influenced by subtle (and not so subtle) factors involving the method of collection (i.e., radiation, temperature, crystal size, measurement times, etc.), it was surmised that data collection under modified conditions might sufficiently perturb the resultant intensities to such an extent that one of the direct methods programs would succeed. However, all of these data collection modifications failed to alleviate the problems encountered in the direct methods structure solution. Although a variety of options were utilized in each of the various programs, application of these options seemed to provide little or no improvement in the solution of this difficult structure over those obtained by simple use of the program default parameters.

By the time the third and fourth data collections had been completed, the absolute structure of phakellistatin 8 had already been determined by alternative methods (as indicated above). Even with this knowledge and despite our best efforts at solving the structure by direct methods, the X-ray structure of phakellistatin 8 defied solution. Since we had expended considerable effort (>200 separate phasing trials using the aformentioned programs), additional attempts at direct method solution were deemed to be impractical and the problem was temporarily deferred. Approximately one year later, the opportunity arose to address the structure problem again with a new, test version of the SIR series of direct methods programs. Surprisingly, solution of the structure was accomplished during a rather routine run of SIR96[20] using data from the fourth data collection. The coordinates of all 82 non-hydrogen atoms of the parent peptide molecule were revealed in the Fourier map, as well as eight solvent atoms. Anisotropic least-squares refinement of the peptide atomic coordinates and isotropic refinement of the solvent atoms proceeded smoothly to yield a standard crystallographic R_1 factor or 0.0631 (2 $\sigma(I)$ cutoff). With the atomic coordinates in hand, successful refinement of the other three data sets was also achieved.

Although new features had been added to SIR96 to facilitate structure solution, curiously none of these new modifications, with one exception, were used in the solution of phakellistatin 8. The one exception was an increase in the number of "strong" reflections initially used (from 499 to 800), which resulted in an increased number of invariant relationships being generated and used in the initial phasing of the SIR program. The consequence of this increased number of reflections (and relationships) was a more accurate determination of the starting phases in the convergence map, thus resulting in a structural solution. The lack of a sufficient number of "strong" reflections being used in the previous convergence mapping programs or as starting phases in random phasing type programs is believed to be the reason for the failure of these programs, which were developed for smaller structure problems.

3. Experimental Section

X-ray Crystal Structure Determination. Phakellistatin 8 (2). Colorless, thick, crystalline plates of the cyclic decapeptide **2** were grown from an aqueous methanol solution and used in the data collections. All collections were performed with an Enraf-Nonius CAD4 diffractometer. In all data collections, linear and anisotropic decay corrections were applied to the intensity data, as well as an empirical absorption correction (based on a series of ψ-scans).[22] Full-matrix least-squares refinement on F^2 (in which the quantity minimized is $\sum_{hkl} w'_{hkl}(|F_o|^2 - |kF_c|^2)^2$) and difference Fourier maps were done with SHELXL-93.[21] A final standard crystallographic residual R_1 (defined as $\sum||F_o| - |F_c||/\sum|F_o|$) and the corresponding Sheldrick R values, wR_2 (based on F^2 and defined as $[\sum[w(F_o^2 - F_c^2)^2]/\sum[w(F_o^2)^2]]$), are reported for each. In addition to the brief discussion below of the four separate data sets, a more detailed summary is included in the Supporting Information.

3.1. Cu Data Collection (Containing Friedel Pairs). The data collection was performed at 298 ± 1 K using a crystal of peptide **2**: dimensions 0.40 × 0.36 × 0.36 mm. Crystal data: $C_{61}H_{88}N_{10}O_{11}\cdot 5^1/_2H_2O\cdot{}^1/_2CH_3OH$, orthorhombic space group $P2_12_12$, with a =

(13) (a) Main, P.; Fiske, S.; Hull, S.; Lessinger, L.; Geramin, G., Declercq, J-P.; Woolfson, M. *Multan-80, A System of Computer Programs for the Automatic Solution of Crystal Structures from X-ray Diffraction Data*; Department of Physics: University of York, York, England, 1980. (b) Jia-Xing, Y. *RANTAN-81, Program for the Automatic Solution of Crystal Structures from X-Ray Diffraction Data by Random Starting Point Tangent Formula*; Depertment of Physics: University of York, York, England, 1980. (c) DeClercq, J.; Germain, G.; Woolfson, M. *Acta Crystallogr.* **1979**, *A35*, 622−626. (d) Hull, S.; Viterbo, D.; Woolfson, M., Shao-Hui, Z. *MAGEX, A Procedure for Phase Determination*; Department of Physics: University of York, York, England, 1980.

(14) Gilmore, C. *Mithril, A Computer Program for the Automatic Solution of Crystal Structures from X-ray Data*, version 1.0; Department of Chemistry: University of Glasgow, Glasgow G12 800, Scotland, 1983.

(15) Sheldrick, G. M. *SHELXS-86, A Program for Solution of Crystal Structure from Diffraction Data*; Institut für Anorganische Chemie der Univ. of Göttingen: Göttingen, Germany, 1986.

(16) Schenk, H. *Simpel, An Interactive Program System for Direct Methods*, version 3.9.9; Laboratory for Crystallography, University of Amsterdam: Amsterdam, The Netherlands, 1989.

(17) Burla, M.; Camalli, M.; Cascarano, G.; Giacovazzo, C.; Polidari, G.; Spagna, R.; Viterbo, D. *J. Appl. Crystallog.* **1989**, *22*, 389−93.

(18) Altomare, A.; Cascarano, G.; Giacovazzo, C.; Guagliardi, A.; Burla, M.; Polidori, G.; Camalli, M. *SIR92 - A Program for Automatic Solution of Crystal Structures by Direct Methods*; Dipartimento Geomineralogico: Univ. of Bari, Italy, 1992.

(19) Egert, E. *PATSEE, Fragment Search by Integrated Patterson and Direct Methods, Compatible with SHELXS-86*; Institut für Anorganische Chemie der Univ. Göttingen: Göttingen, Germany, 1986.

(20) For further details concerning the modifications and improvements implemented into SIR96, contact one of the authors (G.L.C.).

(21) Sheldrick, G. M. *SHELXL-93. Program for the Refinement of Crystal Structures*; Univ. of Göttingen: Germany, 1993.

(22) North, A. C.; Phillips, D. C.; Mathews, F. S. *Acta Crystallogr.* **1968**, *A24*, 351.

20.258(5), b = 24.171(5), c = 13.909(1) Å, V = 6811(2) Å^3, λ (Cu Kα) = 1.54180 Å, ρ_o = 1.205 g m^{-3}, ρ_c = 1.222 g cm^{-3} for Z = 4 and FW = 1252.52, F(000) = 2704. All reflections corresponding to a complete octant, with $2\theta \leq 130°$, were measured using the $\omega/2\theta$ scan technique. The Friedel pair reflection was also collected, whenever possible, after each reflection. A final standard crystallographic residual R_1 of 0.0717 for the observed data (10 080, Friedels included) and 0.0775 for all data (11 074) was obtained. The corresponding Sheldrick R values were 0.1995 and 0.2087, respectively.

3.2. Mo Data Collection. The data collection was performed at 296 ± 1 K using Mo radiation on the same crystal as in section 3.7. Crystal data: a = 20.220(5), b = 24.124(8), c = 13.907(3) Å; V = 6784(3) Å^3; λ (Mo Kα) = 0.71069 Å; ρ_c = 1.226 g cm^{-3}. All reflections corresponding to a complete octant, with $2\theta \leq 50°$, were measured, using the $\omega/2\theta$ scan technique (6568 unique reflections which were collected). A total of 3741 reflections were considered observed ($I_o > 2\sigma(I_o)$) and were used in the subsequent refinement. A standard crystallographic residual R_1 of 0.0785 was obtained for the observed data (0.1351 for all data). The corresponding Sheldrick R values were wR_2 of 0.1942 and 0.2419.

3.3. Cu Low-Temperature Data Collection. The data collection was performed at 244 ± 1 K using Cu radiation on a new crystal of peptide **2**: dimensions 0.30 × 0.24 × 0.20 mm. Crystal data: a = 20.164(5), b = 24.059(7), c = 13.845(4) Å; V = 6716(3) Å^3; λ (Cu Kα) = 1.54180 Å; ρ_c = 1.239 g cm^{-3}. A total of 5516 reflections were collected (slightly more than a complete octant), of which 5484 were unique reflections. A total of 3752 reflections were considered observed and were used in the subsequent refinement. Refinement yielded a standard crystallographic residual R_1 of 0.0826 for the observed data, 0.1181 for all data. The corresponding Sheldrick R values were wR_2 of 0.2031 and 0.2360, respectively.

3.4. Extended Cu Data Collection. The data collection was performed at 296 ± 1 K using Cu radiation on another crystal of **2**: dimensions 0.46 × 0.40 × 0.34 mm. Crystal data: a = 20.294(2), b = 24.141(6), c = 13.903(3) Å; V = 6811(2) Å^3; λ (Cu Kα) = 1.54180 Å; ρ_c = 1.221 g cm^{-3}. A complete hemisphere of reflections was collected resulting in 10 874 unique reflections. Of these, 10 061 reflections were considered observed and were used in the subsequent refinement. Refinement yielded a standard crystallographic residual R_1 of 0.0631 for the observed data, 0.0704 for all data. Sheldrick R values were wR_2 of 0.1723 and 0.1825.

3.5. Merged Room-Temperature Data Refinement. The three room-temperature (~296 ± 2 K) data collections described above in sections 3.1, 3.2, and 3.4, after data reduction and absorption corrections, were merged to yield 10 603 unique reflections, of which 10 603 were considered observed. Refinement of this merged data set resulted in an R_1 of 0.0651 for the observed data, 0.0718 for all data. Corresponding Sheldrick R values were wR_2 of 0.1749 and 0.1805. Final difference Fourier maps showed minor residual electron density remaining with the largest peak of 0.58 e/Å^3 and hole of −0.40 e/Å^3. The results of this merged refinement are presented in Tables 1−4.

3.6. Structure Solution and Refinement. A solution to all of the previously described data collections was finally realized with SIR96, in which coordinates were obtained for all non-hydrogen atoms of the decapeptide molecule during a program run in which NREF was set at 800 and default values for RANDOM phasing were used. Subsequent difference Fourier maps revealed additional, extensive solvation of the parent decapeptide in the unit cell. In addition to intramolecular hydrogen bonding, considerable intermolecular solvate H-bonding was identified between the parent peptide molecule, six molecules of water and one molecule of the solvent, methanol (see Figure 1[23]). In addition, some rather unique features which were initially difficult to interpret were also revealed. One of these involved the oxygen atom of one of the water molecules, W-1, which was determined to occupy a special position requiring an occupancy of 0.5. W-1 is also H-bonded to another oxygen atom, O-SO (W-1···O-SO distance, 2.82Å). The O-SO atom is a constituent of the hydroxyl portion of a molecule of methanol (e.g., bond distance for C-SO···O-SO is 1.37 Å). Because the carbon atom of methanol, i.e., C-SO, also occupied a special position requiring an occupancy of 0.5, this implied that the hydroxyl atom O-SO likewise has an occupancy of 0.5. If the methanol hydroxyl is disordered equally over the two, symmetry-equivalent sites (see Figure 1) this would be feasible. As a result, we have assigned 0.5 occupancy to the general positions occupied by O-SO.

Table 1. Merged Room-Temperature Crystal Data Collections and Solution and Structure Refinement of Phakellistatin 8 (**2**)

empirical formula	$C_{61}H_{88}N_{10}O_{11}\cdot5^1/_2\ H_2O\cdot{}^1/_2CH_3OH$
formula weight	1252.52
temperature	296(2) K
wavelength	1.54180 Å
crystal system	orthorhombic
space group	$P2_12_12$
unit cell dimensions	a = 20.294(2) Å, α = 90.00° b = 24.141(6) Å, β = 90.00° c = 13.903(3) Å, γ = 90.00°
volume	6811(2) Å^3
Z	4
F(000)	2704
crystal description	thick plates
crystal color	colorless
crystal size	0.46 × 0.40 × 0.34 mm
density (calculated)	1.221 mg/m^3
density (observed)	1.205 mg/m^3
absorption coefficient	0.734 mm^{-1}
instrument	Enraf-Nonius CAD4 diffractometer
radiation source	fine-focus sealed tube
monochromator	graphite
θ range for data collection	2.84−66.43°
scan type	$\omega/2\theta$
no. of standards	3
standard interval	60 min
standard decay	−0.2%
index ranges	$-23\leq h\leq 24$, $-28\leq k\leq 28$, $-16\leq l\leq 16$
reflections collected	40266
independent reflections	11746 [R(int) = 0.1283]
absorption correction(s)	semiempirical ψ-scan
max. and min. transmission(s)	0.9979 and 0.9018 (ψ scan)
reflections observed	10603
observed criterion	$>2\sigma(I)$
solution software	SIR96
refinement software	SHELXL-93 (Sheldrick, 1993)
graphics software	SHELXTL-PLUS
publication software	SHELXL-93
refinement method	full least-squares on F^2
refinement weighting scheme	calc $w = 1/[\sigma^2(F_o^2)+(0.1147P)^2+1.2284P]$ where $P=(F_o^2+2F_c^2)/3$
H atom coordinates solution	geometry calc
H atoms least-squares treatment	riding-fixed at 1.5 Uiso of attached atom
Data/restraints/parameters	11735/9/768
goodness-of-fit on F^2	1.046 obs, 1.013 all
final ls shift esd's	0.001 mean, 0.013 max
final R indices [$I>2\sigma$(I)]	R_1 = 0.0651, wR_2 = 0.1749
R indices (all data)	R_1 = 0.0718, wR_2 = 0.1805
extinction coefficient	0.00085(14)
extinction method	SHELXL
extinction expression	$F_c^*=kF_c[1+0.001\times F_c^2\lambda^3/\sin(2\theta)]^{-1/4}$
absolute structure details	Flack, H. D. *Acta Crystallogr.* **1983**, *A39*, 876-881
Flack parameter	−0.04(20)
largest diff. peak and hole	0.580 and −0.405 eA^{-3}

3.7. Absolute Configuration. The final structure of phakellistatin 8 agreed with that previously proposed from NMR data interpretations.[12] Thus, the cyclodecapeptide sequence has been determined to be cyclo-[Pro$_1$-Pro$_2$-Ile$_3$-Phe$_4$-Val$_5$-Leu$_6$-Pro$_7$-Pro$_8$-Tyr$_9$-Ile$_{10}$]. Although the Flack parameter obtained (−0.04, esd 0.20) for the model shown in Figure 1 would suggest that the absolute stereochemistry assignments are correct, it is certainly not conclusive (nor should it be expected to be, since the anomalous dispersion of oxygen is very weak). However, the absolute stereochemical assignment of all chiral atoms in phakellistatin 8 could be readily assigned by correlation with the constituent, natural L-amino acids, the presence and absolute stereochemistry of which had previ-

(23) Preparation of Figure 1 was done with SHELXTL-PLUS (G. Sheldrick, Siemens Analytical X-Ray Instruments, Inc., Madison, WI 53719).

Table 2. Atomic Coordinates ($\times 10^4$) and Equivalent Isotropic Displacement Parameters ($Å^2 \times 10^3$) for Phakellistatin 8[a]

atom	*x*	*y*	*z*	*U*(eq)	atom	*x*	*y*	*z*	*U*(eq)
N_1	5255(1)	2375(1)	4799(2)	47(1)	C_6^{γ}	9774(2)	4047(2)	1977(4)	82(1)
C_1'	5651(2)	2663(1)	6380(2)	48(1)	$C_6^{\delta 1}$	10125(3)	4158(2)	2945(5)	110(2)
O_1'	5781(2)	2183(1)	6560(2)	76(1)	$C_6^{\delta 2}$	10243(4)	4086(4)	1116(6)	153(3)
C_1^{α}	5196(2)	2810(1)	5538(2)	47(1)	N_7	9039(1)	2437(1)	635(2)	43(1)
C_1^{β}	4465(2)	2772(2)	5844(3)	66(1)	C_7'	8927(1)	1586(1)	1571(2)	41(1)
C_1^{γ}	4134(2)	2410(2)	5123(4)	93(2)	O_7'	9392(1)	1714(1)	2079(2)	57(1)
C_1^{δ}	4657(2)	2033(2)	4766(3)	67(1)	C_7^{α}	8844(1)	1855(1)	586(2)	42(1)
N_2	5885(1)	3083(1)	6920(2)	42(1)	C_7^{β}	9322(2)	1608(1)	−152(2)	62(1)
C_2'	6111(1)	4008(1)	6168(2)	39(1)	C_7^{γ}	9812(3)	2015(2)	−334(6)	38(3)
O_2'	6008(1)	4509(1)	6101(2)	52(1)	C_7^{δ}	9619(2)	2558(1)	28(3)	59(1)
C_2^{α}	5702(1)	3666(1)	6866(2)	40(1)	N_8	8474(1)	1210(1)	1851(2)	43(1)
C_2^{β}	5817(2)	3876(1)	7903(2)	49(1)	C_8'	7297(1)	1251(1)	1279(2)	45(1)
C_2^{γ}	6381(2)	3515(2)	8259(2)	60(1)	O_8'	6800(1)	1008(1)	1015(2)	74(1)
C_2^{δ}	6234(2)	2954(1)	7826(2)	56(1)	C_8^{α}	7961(2)	948(1)	1267(2)	47(1)
N_3	6578(1)	3752(1)	5671(2)	46(1)	C_8^{β}	7901(2)	375(1)	1714(3)	68(1)
C_3'	6785(1)	4151(1)	4045(2)	44(1)	C_8^{γ}	8018(2)	496(2)	2784(3)	73(1)
O_3'	6888(1)	4600(1)	3660(2)	58(1)	C_8^{δ}	8553(2)	927(2)	2782(2)	62(1)
C_3^{α}	7045(2)	4057(1)	5070(2)	47(1)	N_9	7301(1)	1777(1)	1549(2)	42(1)
C_3^{β}	7722(2)	3768(2)	5087(3)	62(1)	C_9'	6182(2)	2039(1)	2120(2)	52(1)
$C_3^{\gamma 1}$	7995(2)	3711(2)	6105(3)	86(1)	O_9'	5615(1)	2153(2)	1922(3)	108(1)
$C_3^{\gamma 2}$	8199(2)	4056(2)	4398(4)	96(2)	C_9^{α}	6745(1)	2151(1)	1410(2)	44(1)
C_3^{δ}	8088(5)	4229(4)	6651(6)	171(4)	C_9^{β}	6493(2)	2176(1)	366(2)	53(1)
N_4	6505(1)	3720(1)	3610(2)	48(1)	C_9^{γ}	7044(2)	2249(1)	−354(2)	49(1)
C_4'	6618(2)	3794(1)	1795(2)	49(1)	$C_9^{\delta 2}$	7177(2)	1845(1)	−1035(3)	61(1)
O_4'	6487(2)	3535(1)	1053(2)	78(1)	$C_9^{\delta 1}$	7418(2)	2729(1)	−380(2)	50(1)
C_4^{α}	6170(2)	3727(1)	2673(2)	49(1)	$C_9^{\epsilon 2}$	7662(2)	1919(2)	−1715(3)	76(1)
C_4^{β}	5620(2)	4164(2)	2599(3)	64(1)	$C_9^{\epsilon 1}$	7900(2)	2818(2)	−1065(2)	56(1)
C_4^{γ}	5051(2)	4086(2)	3264(2)	57(1)	C_9^{ζ}	8019(2)	2407(2)	−1744(2)	65(1)
$C_4^{\delta 2}$	4501(2)	3779(3)	3005(3)	112(2)	O_9^{η}	8490(2)	2466(2)	−2461(2)	95(1)
$C_4^{\delta 1}$	5048(2)	4314(2)	4171(3)	61(1)	N_{10}	6358(1)	1848(1)	2973(2)	57(1)
$C_4^{\epsilon 2}$	3962(2)	3742(3)	3615(4)	117(2)	C_{10}'	5823(2)	2299(1)	4344(2)	45(1)
$C_4^{\epsilon 1}$	4504(2)	4269(2)	4769(3)	71(1)	O_{10}'	6286(1)	2629(1)	4423(2)	55(1)
C_4^{ζ}	3958(2)	4007(2)	4478(3)	86(1)	C_{10}^{α}	5889(2)	1769(1)	3752(2)	51(1)
N_5	7119(1)	4155(1)	1851(2)	47(1)	C_{10}^{β}	6088(2)	1279(2)	4411(3)	74(1)
C_5'	8103(2)	4093(1)	763(2)	54(1)	$C_{10}^{\gamma 1}$	6775(2)	1333(2)	4823(3)	92(2)
O_5'	8394(2)	4222(2)	27(2)	103(1)	$C_{10}^{\gamma 2}$	5987(4)	728(2)	3882(7)	140(3)
C_5^{α}	7446(2)	4370(1)	994(2)	48(1)	C_{10}^{δ}	6911(4)	941(4)	5652(7)	173(4)
C_5^{β}	7533(2)	5005(1)	1070(2)	59(1)	W-1[b]	5000	5000	7194(3)	70(1)
$C_5^{\gamma 1}$	8001(3)	5170(2)	1877(3)	81(1)	W-2	4372(2)	1718(2)	2273(3)	107(1)
$C_5^{\gamma 2}$	6863(2)	5293(2)	1170(3)	78(1)	W-3	7693(4)	2292(3)	3594(6)	185(2)
N_6	8334(1)	3720(1)	1383(2)	48(1)	W-4	9342(6)	4274(4)	−1360(9)	248(4)
C_6'	8717(1)	2784(1)	1206(2)	43(1)	W-5	5000	5000	9697(10)	156(4)
O_6'	8259(1)	2628(1)	1736(2)	49(1)	W-6	5411(4)	5268(3)	9069(5)	98(2)
C_6^{α}	8922(1)	3391(1)	1228(2)	48(1)	C-SO[b]	7379(6)	2532(5)	5863(9)	276(5)
C_6^{β}	9429(2)	3493(1)	2029(3)	61(1)	O-SO[b]	5789(9)	270(8)	1144(14)	377(8)

[a] *U*(eq) is defined as one third of the trace of the orthogonalized U_{ij} tensor. [b] Atoms present at $^1/_2$ occupancy.

ously been established and reported.[12] Thus, the chiral atoms (using the numbering shown in Figure 1) C1A, C2A, C3A, C3B, C4A, C5A, C6A, C7A, C8A, C9A, C10A, and C10B are all of the *S* configuration.

4. Results and Discussion

4.1. Crystal Conformation. Fractional coordinates for all non-hydrogen atoms of phakellistatin 8 (**2**) are listed in Table 2. Table 3 contains a listing of all bond lengths and angles for phakellistatin 8. Bond distances were within generally accepted limits,[24] with the exception of the $C^{\beta}-C^{\gamma}$ and the $C^{\gamma}-C^{\delta}$ bonds of Pro_1 (1.490 and 1.485 Å) and Pro_7 (1.420 and 1.446 Å) residues, and the $C^{\gamma}-C^{\delta}$ bond of Ile_3 (1.475 Å). In each case, bond lengths consistently refined to shorter values than were initially expected (~1.52 Å), even when bond restraints were applied during refinement. The estimated standard deviations for the bond lengths of the proline residues were all in the order of 0.003−0.006. Although it is well known that calculated least-squares esd values are often underestimated,[25] it is believed that the apparent shortening of the $C^{\beta}-C^{\gamma}$ and the $C^{\gamma}-C^{\delta}$ bonds in Pro_1 and Pro_7 are statistically significant. Similar bond shortening of these same bonds was also observed in the lower temperature (244 K) data collection of phakellistatin 8, although slightly less pronounced. (See Table 3). In addition, such prolyl residue bond-shortening phenomena have previously been reported by a number of researchers[7c,26] in other oligopeptide structures.

In nearly every occurrence of proline bond shortening at the $C^{\beta}-C^{\gamma}$ and the $C^{\gamma}-C^{\delta}$ bonds reported, an accompanying increase in the $C^{\beta}-C^{\gamma}-C^{\delta}$ bond angle has also been observed. This angle widening is observed in phakellistatin 8 as well, particularly for Pro_7, which increases from a nominal value of ~104.1° to 111.8°. The bond shortening (and concomitant angle expansion) phenomenon was first observed in several early, proline-containing X-ray crystal structures[7c,26a−d] and a logical

(24) (a) Ramachandran, G.; Kolaskar, A.; Ramakrishnan, C. *Biochim. Biophys. Acta* **1974**, 298−302. (b) Benedetti, E. In *Peptides, Proceedings of the Fifth American Symposium*; Goodman, M., Meienhofer, J., Eds.; John Wiley & Sons: New York, NY, 1977; pp 257−76. (c) Ashida, T.; Tsunogae, Y.; Tanaka, I.; Yamane, T. *Acta Crystallogr.* **1978**, *B43*, 212−218. (d) Allen, F.; Kennard, O.; Watson, D.; Brammer, L.; Orpen, A.; Taylor, R. *J. Chem. Soc., Perkin Trans. 2* **1987**, S1−S19. (e) Lamba, S.; Scatturin, A.; Ughetto, G. *Biopolymers* **1989**, *28*, 409−20. (f) Bhandary, K.; Kopple, K. *Acta Crystallogr.* **1991**, *C47*, 1483−7. (g) Eggleston, D.; Baures, P.; Peishoff, C.; Kopple, K. *J. Am. Chem. Soc.* **1991**, *113*, 4410−6. (h) Morita, H.; Kayashita, T.; Takeya, K.; Itokawa, H.; Shiro, M. *Tetrahedron. Lett.* **1995**, *51* (46), 12539−48.

(25) Jones, P. *Chem. Soc. Rev.* **1984**, *13* (2), 157−72.

Table 3. Bond Lengths (Å) and Angles (deg) for Phakellistatin 8[a] (**2**)

	Pro_1	Pro_2	Ile_3	Phe_4	Val_5	Leu_6	Pro_7	Pro_8	Tyr_9	Ile_{10}	mean
					Bonds						
$N_i-C_i^\alpha$	1.474(4)	1.456(4)	1.461(4)	1.469(4)	1.460(4)	1.449(4)	1.461(4)	1.464(4)	1.459(3)	1.454(4)	1.461(4)
$C_i^\alpha-C_i'$	1.533(4)	1.522(4)	1.536(4)	1.531(4)	1.527(4)	1.523(4)	1.524(4)	1.533(4)	1.534(4)	1.528(4)	1.529(4)
$C_i'-O_i'$	1.213(4)	1.233(3)	1.226(3)	1.235(4)	1.222(4)	1.245(3)	1.229(3)	1.223(4)	1.213(4)	1.236(4)	1.227(4)
$C_i'-N_{i+1}$	1.350(4)	1.334(4)	1.331(4)	1.341(4)	1.332(4)	1.325(4)	1.350(4)	1.323(4)	1.322(4)	1.327(4)	1.333(4)
$C_i^\alpha-C_i^\beta$	1.546(5)	1.545(4)	1.542(4)	1.540(4)	1.546(4)	1.536(5)	1.532(4)	1.521(4)	1.540(4)	1.551(5)	
$C_i^\beta-C_i^\gamma$	1.490(5)	1.521(5)	1.526(6)	1.492(5)	1.522(5)	1.511(5)	1.420(6)	1.534(6)	1.511(4)	1.512(7)	
			1.529(6)		1.533(5)					1.532(8)	
	{1.498(12)	1.523(12)}[b]					{1.474(12)	1.52(2)}[b]			
$C_i^\gamma-C_i^\delta$	1.485(6)	1.510(5)	1.475(8)	1.377(5)		1.532(8)	1.446(6)	1.502(5)	1.385(5)	1.551(5)	
				1.386(6)		1.546(7)			1.386(5)		
	{1.498(12)	1.524(13}[b]					{1.489(12)	1.503(12)}[b]			
$C_i^\delta-C_i^\epsilon$				1.388(7)					1.382(5)		
				1.386(5)					1.376(5)		
$C_i^\epsilon-C_i^\zeta$				1.339(6)					1.385(6)		
				1.358(7)					1.390(5)		
$N_i-C_i^\delta$	1.467(4)	1.478(4)					1.477(4)	1.473(4)			
$C_i^\zeta-O_i^\eta$									1.389(4)		
					Angles						
$C_{i-1}'N_iC_i^\alpha$	120.0(4)	127.4(2)	121.8(2)	126.3(2)	121.9(3)	124.3(2)	120.2(2)	128.0(2)	123.4(2)	122.4(3)	123.6(2)
$N_{i+1}C_i'C_i^\alpha$	117.6(2)	118.1(2)	116.9(2)	118.2(3)	117.9(2)	119.1(2)	118.0(2)	117.2(2)	115.9(2)	116.6(2)	117.6(2)
$N_iC_i^\alpha C_i'$	108.6(2)	114.7(2)	112.5(2)	115.7(2)	114.3(2)	107.7(2)	109.7(2)	114.4(2)	112.5(2)	110.5(2)	112.1(2)
$C_i^\alpha C_i'O_i'$	120.7(3)	119.3(2)	118.6(3)	119.0(3)	119.0(3)	119.1(3)	119.0(2)	119.9(3)	119.5(3)	121.3(3)	119.5(3)
$N_{i+1}C_i'O_i'$	121.7(3)	122.7(3)	124.4(3)	122.7(3)	123.0(3)	121.9(3)	122.0(3)	123.3(3)	122.6(3)	122.0(3)	122.6(3)
$C_i'C_i^\alpha C_i^\beta$	110.7(3)	109.5(2)	112.7(2)	107.7(3)	110.4(3)	110.6(2)	111.5(2)	111.1(3)	111.5(2)	110.1(3)	
$N_iC_i^\alpha C_i^\beta$	103.2(2)	103.3(2)	110.0(2)	113.7(3)	110.5(2)	110.9(2)	103.5(2)	102.9(2)	114.0(2)	111.6(3)	
$C_i^\alpha C_i^\beta C_i^\gamma$	106.4(3)	103.3(2)	112.3(3)	115.7(3)	112.4(3)	114.6(3)	107.1(3)	102.2(3)	112.6(2)	113.4(3)	
			110.4(3)		110.7(3)					110.1(5)	
$C_i^\beta C_i^\gamma C_i^\delta$	105.1(3)	103.6(3)	116.6(5)	121.3(3)		109.0(4)	111.8(3)	104.0(3)	121.3(3)	113.7	
				122.0(3)		112.4(4)			120.9(3)		
$C_i^\gamma C_i^\delta C_i^\epsilon$				121.4(3)					122.3(3)		
				120.6(4)					121.2(4)		
$C_i^\delta C_i^\epsilon C_i^\zeta$				121.0(4)					118.7(3)		
				121.0(4)					120.2(3)		
$C_i^\gamma C_i^\beta C_i^\gamma$			113.0(4)		111.6(4)					112.4(4)	
$C_i^\delta C_i^\gamma C_i^\delta$				116.6(3)		112.5(4)			117.7(3)		
$C_i^\epsilon C_i^\zeta C_i^\epsilon$				118.9(4)					119.8(3)		
$O_i^\eta C_i^\zeta C_i^\epsilon$									122.3(4)		
									117.9(4)		
$C_i^\gamma C_i^\delta N_i$	103.7(3)	104.2(2)					103.6(3)	104.2(3)			
$C_i^\delta N_iC_i^\alpha$	110.7(2)	111.7(2)					112.2(2)	111.3(2)			
$C_i^\delta N_iC_{i-1}'$	128.8(2)	119.0(2)					127.5(3)	119.5(2)			

[a] Data are for the three merged room-temperature data sets. Esd's in parentheses. [b] Bond lengths for **2** from low-temperatre (244 K) Cu data collection.

explanation for this phenomenon seems to have first been proposed by Ashida and Kakudo,[26e] based upon the conformational flexibility of the pyrrolidine ring. Such ring flexibility is due to the displacement of the C^β and C^γ atoms out of the mean plane defined by the five atoms in the ring. These displacements assume a continuous range of values and, as a consequence, give rise to disorder in a direction perpendicular to the plane of the ring. Confirmatory experimental evidence for such disorder is found in the highly anisotropic thermal vibration ellipsoids often displayed by the C^β and C^γ atoms, with the principal axis of the ellipsoids being nearly perpendicular to the mean plane of the five-membered ring. The net effect is that the perceived bond distances for the $C^\beta-C^\gamma$ and the $C^\gamma-C^\delta$ bonds appear shorter than normal, resulting in a wider $C^\beta-C^\gamma-C^\delta$ angle. The anisotropic nature of the thermal ellipsoids for the C^β and C^γ atoms of the two Pro-Pro segments in phakellistatin 8 is shown in Figure 2. Highly anisotropic thermal vibrations perpendicular to the pyrrolidine rings are particularly evident for the γ carbon atoms of Pro_1 and Pro_7 (C1G and C7G); the principal mean square thermal displacement U values for these two atoms are 0.16, 0.06, and 0.05 Å^2 for C1G, and 0.31, 0.07, and 0.04 Å^2 for C7G. These thermal displacement values are reduced to 0.12, 0.04, and 0.03 Å^2 for C1G and 0.24, 0.05, and 0.02 for C7G in the low-temperature data collection, consistent with the decreased thermal motion of the proline rings at the lower temperature.

Since the bond-shortening process seemed to be occurring at the N terminal ends of each of the two Pro-Pro peptide units in phakellistatin 8, bond distances about the C^γ atom reported for the proline pairs in antamanide 3 were also examined to see if a similar phenomenon was occurring. Although there was some indication that such effects might occur in antamanide as well, as exhibited particularly by increased bond angles around the C^γ atoms for the N terminal units of the proline pairs (e.g., 113° and 115° in Pro_2 and Pro_7, respectively), the much larger esd values for the bond lengths (~0.025 Å) and angles (1.6°) reported for this crystal structure[3r] made any conclusions tenuous at best.

(26) (a) Jain, S.; Sobell, M. *J. Mol. Biol.* **1972**, *68*, 1−20. (b) Ueki, T.; Ashida, T.; Kakudo, M.; Sasada, Y.; Katsube, Y. *Acta Crystallogr.* **1969**, *B25*, 1840−9. (c) Matsuzaki, T. *Acta Crystallogr.* **1974**, *B30*, 1029−36. (d) Kartha, G.; Ambady, G. *Acta Crystallogr.* **1975**, *B31*, 2035−9. (e) Ashida, T.; Kakudo, M. *Bull. Chem. Soc. Jpn.* **1974**, *47* (5), 1129−33. (f) Druyan, M.; Coulter, C.; Walter, R.; Kartha, G.; Ambady, G. *J. Am. Chem. Soc.* **1976**, *98* (18), 5496−502. (g) Tanaka, I.; Ashida, T. *Acta Crystallogr.* **1979**, *B35*, 110−4. (h) Marsh, R. *Acta Crystallogr.* **1980**, *B36*, 1265−67. (i) Nair, C.; Vijayan, M., J. *Indian Inst. Sci.* **1981**, *61*, 81−103. (j) Benedetti, E.; Bavoso, A.; Blasio, B.; Pavone, V.; Pedone, C.; Toniolo, C.; Bonora, G. *Biopolymers* **1981**, *22*, 305−17. (k) Nakashima, T.; Yamane, T.; Tanaka, I.; Ashida, T. *Acta Crystallogr.* **1984**, *C40*, 171−4.

Table 4. Torsion Angles (deg) for Phakellistatin 8 and Antamanide

	phakellistatin 8									
	Pro_1	Pro_2	Ile_3	Phe_4	Val_5	Leu_6	Pro_7	Pro_8	Tyr_9	Ile_{10}
ϕ_i	−65	−90	−88	71	−101	−118	−62	−92	75	−88
ψ_i	153	1	−45	−41	−5	146	143	20	31	153
ω_i	7	−173	174	−161	175	179	11	167	174	167
χ_i^{11}	−12	31	−57	−64	65	−73	11	35	−48	56
χ_i^{12}			176		−60					−71
χ_i^{21}	28	−38	−59	89		165	−14	−39	−66	165
χ_i^{22}						−69				
χ_i^{3}	−33	30					14	27		
χ_i^{4}	27	−11					−5	−5		
χ_i^{5}	−9	−12					−3	−20		

	antamanide									
	Val_1	Pro_2	Pro_3	Ala_4	Phe_5	Phe_6	Pro_7	Pro_8	Phe_9	Phe_{10}
ϕ_i	−113	−64	−79	−103	70	−78	−62	−92	−101	56
ψ_i	158	161	−20	−22	29	161	160	−4	−22	48
ω_i	178	2	−165	172	176	168	4	−177	174	178
χ_i^{11}	−62	−14	25		−52	−70	11	29	−70	−50
χ_i^{12}	64									
χ_i^{21}		25	−33		−90	−32	−11	−31	−24	−83
χ_i^{22}										
χ_i^{3}		−26	27				6	22		
χ_i^{4}		15	−10				3	−4		
χ_i^{5}		−1	−9				−10	−16		

Average backbone bond distances and angles for phakellistatin 8 are listed in Table 3. Averaged over the 10 residues, the mean values are 1.461 Å for $N_i-C_i^{\alpha}$, 1.529 Å for $C_i^{\alpha}-C_i'$, 1.227 Å for $C_i'-O_i'$, 1.333 Å for $C_i'-N_{i+1}$ and 123.6° for $C_{i-1}'-N_i-C_i^{\alpha}$, 117.6° for $N_{i+1}-C_i-C_i^{\alpha}$, 112.1° for $N_i-C_i^{\alpha}-C_i'$, 119.5° for $C_i^{\alpha}-C_i'-O_i'$, and 122.6° for $N_{i+1}-C_i'-O_i'$. These values agree well with the average values which have been previously reported for cyclic peptides,[24a,c,e−h] indicating little or no strain in the cyclic framework.

A comparison of conformational angles for the crystal structures of phakellistatin 8 (**2**) and antamanide (**1**) is shown in Table 4. The crystal structure of phakellistatin 8 contains all-trans peptide bonds, except for the cis peptide bonds at the Pro_1-Pro_2 ($\omega_1 = 7°$) and the Pro_7-Pro_8 ($\omega_7 = 11°$) linkages. Similar results were observed for antamanide, which also has cis peptide conformations ($\omega_2 = 2°$, $\omega_7 = 4°$) at the Pro_2-Pro_3 and Pro_7-Pro_8 amide bonds. For phakellistatin 8, the presence of the two Pro-Pro moieties comprising the I+1 and I+2 peptide residues involved in the two major turns in the macrocyclic peptide ring allows the overall peptide backbone to assume an elongated, saddlelike conformation, as shown in Figure 3. The conformation is remarkably similar to the crystal structure conformation exhibited by uncomplexed antamanide[7d,e,g−j] (**1**), the peptide backbone of which is also displayed in Figure 3. Again, the presence of two Pro-Pro units in antamanide delineates the second and third residues involved in the peptide backbone reversals. Such conformational turns caused by the presence of an X-Pro peptide sequence are well known,[7j,10b,11a,25a,b,27] and the involvement of proline in various types of turns has been extensively studied.[11b,26i,28] For example, in the $(X\text{-Pro-Y})_2$ cyclic peptide series, it has been noted that the proline residue has a strong preference for the I+1 position of a β-turn.[11a,b,28b] Primarily, this is due to the sterically restricted ϕ and ψ space available to the prolyl residue (caused by the pyrrolidine ring), which in turn causes a favorable orientation of the I+3 amide hydrogen to form an I+3 → hydrogen bond of either a type I or a type II turn. The presence of a cis Pro-Pro sequence offers further inducement to producing a turn. When a cis Y-Pro sequence occurs in proteins, the prolyl residue almost invariably is found to occur in the third position of a type VI β-turn.[11b] Thus, the cis Pro-Pro sequence seems to provide the ideal structural features required for chain reversals in peptides and proteins. Finally, it should be emphasized that although the presence of the two cis Pro-Pro units obviously plays a crucial role in producing grossly similar conformations for the two molecules, the relative peptide backbone positions of the two Pro-Pro linkages in these peptides are not identical. In antamanide (**1**), the Pro-Pro units are on exactly opposing sides of the peptide ring, whereas, in the phakellistatin 8 (**2**) molecule, the proline units are offset by one amino acid unit. As a result, the types of turns involving the Pro-Pro groups might be expected to be slightly different for the two molecules.

In addition to the obvious influence of the cis Pro-Pro linkages on the overall macrocyclic ring conformation, other factors, such as solvation affecting inter- and intramolecular hydrogen bonding[3,7h,8a,b,e,f,i] and metal cation complexation[3,7b−h,8b,29] have been shown to exert considerable control on the crystalline conformation of antamanide and its structurally related analogs. For example, complexation of antamanide with the Li^+ ion results in an even tighter saddle- or cuplike conformation. The latter tighter conformation can be achieved by drawing the two proline pairs toward each other and into the center of the decapeptide ring via rotation about the peptide backbone bonds on the sides of the saddle. Whether such stable complex formation with metal cations and analogous conformational changes can occur with phakellistatin 8 has yet to be determined.

A conformational backbone summary of both molecules is presented in Figure 4 as a Ramachandran plot. All backbone dihedral angles for phakellistatin 8 (**2**) fall within normal, low-energy regions except for two amino acid residues, Phe_4 and Tyr_9, the side chains of which are found to fold back over the peptide backbone. The Ramachandran plot shows the Phe_4 residue ($\phi,\psi = 71°, -41°$) occupying a region normally disallowed for amino acids containing a long side chain. In addition, the Tyr_9 residue ($\phi,\psi = 75°, 31°$) of phakellistatin 8 resides near the high-energy, left-handed α-helical region. Although theoretically possible, left-handed α-helices are generally not energetically favorable for L-amino acids because of the close contact which often results between the amino acid side chain and the peptide backbone.[30] While this general rule is normally applied to linear peptides, it is violated on occasion for cyclic peptides. For example, left-handed α-helix formation has been observed previously in our laboratories for the cycloheptapeptide, stylopeptide 1.[31] In the case of antamanide (**1**), inspection of the plot reveals that the Phe_5 and Phe_{10} residues also occupy the left-handed α-helical region. With phakellistatin 8, the aromatic side chains of these two residues were again found to be folded back over the peptide backbone. A common

(27) (a) Boussard, G.; Marraud, M.; Aubry, A. *Biopolymers* **1979**, *18*, 1297−1331. (b) Creighton, T. In *Proteins, Structures and Molecular Principles*; W. H. Freeman and Company: New York, NY, 1983; pp 236−7.

(28) (a) Chou, P.; Fasman, G. *J. Mol. Biol.* **1977**, *115*, 135−75. (b) Kolaskar, A.; Ramabrahman, V.; Soman, K. *Int. J. Peptide Protein Res.* **1980**, *16*, 1−11. (c) Richardson, J. The Anatomy and Taxonomy of Protein Structure. In *Advances in Protein Chemistry*; Academic Press: New York, NY, 1981; Vol. 34, pp 167−339. (d) Kartha, G.; Aimoto, S.; Varughese, K. *Int. J. Peptide Protein Res.* **1986**, *27*, 112−7.

(29) Ovchinnikov, Y. *Glas. Hem. Drus., Beograd* **1977**, *42* (6−7), 443−62.

(30) Reference 27b, p. 172.

(31) (a) Pettit, G.; Srirangam, J;, Herald, D.; Xu, J-P.; Boyd, M.; Cichacz, Z.; Kamano, Y.; Schmidt, J.; Erickson, K. *J. Org. Chem.* **1995**, *60* (25), 8257−61. (b) Srirangam, J.; Pettit, G.; Herald, D.; Williams, M. *J. Nat. Prod.*, **1997**, submitted.

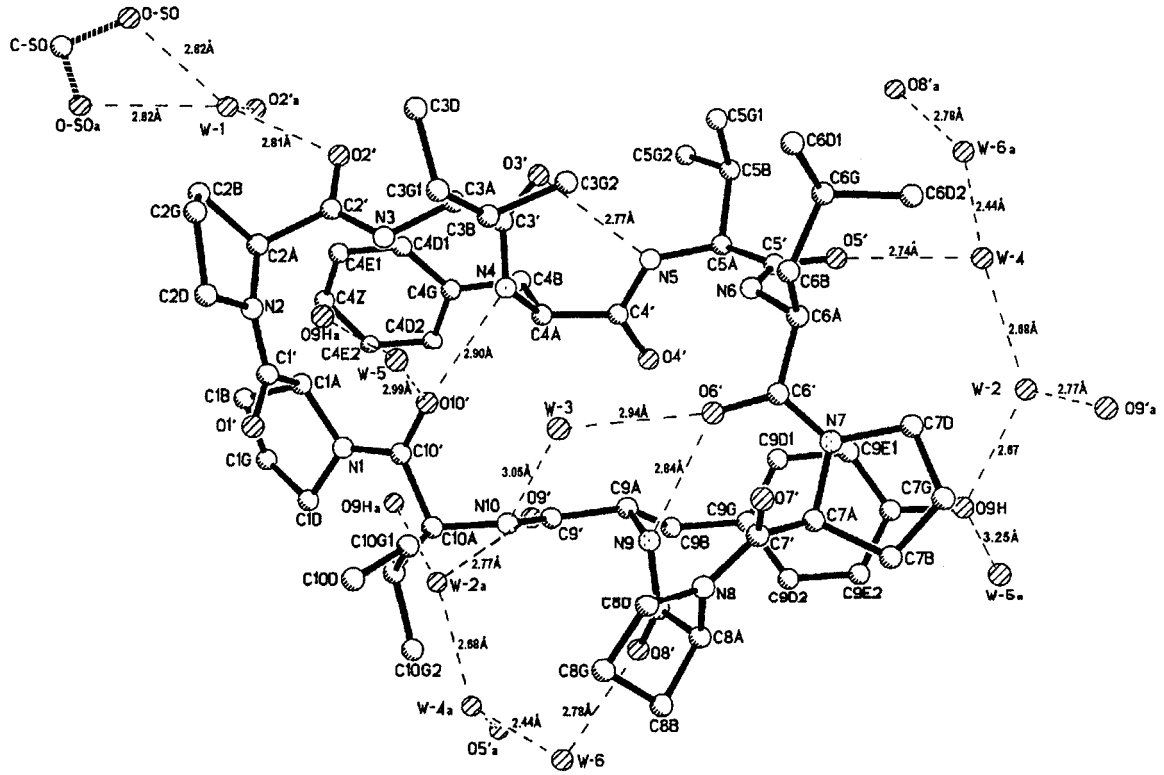

Figure 1. X-ray crystal structure of phakellistatin 8 (**2**) + water and solvent molecules (less hydrogens). Hydrogen bonding is indicated by dashed lines.

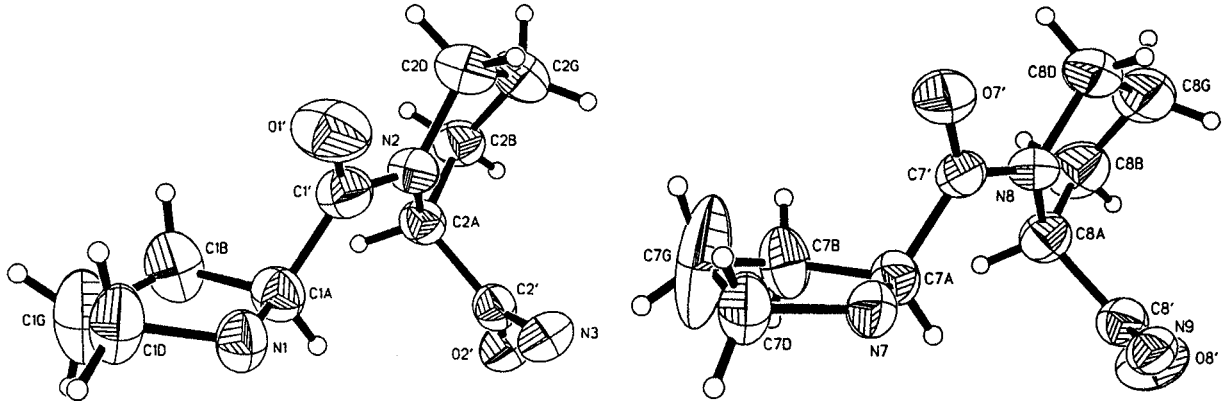

Figure 2. The Pro_1-Pro_2 and Pro_7-Pro_8 segments of phakellinstatin 8 (**2**) showing the elongated thermal ellipsoids (50% probability) for the C^γ atoms (i.e., C1G and C7G).

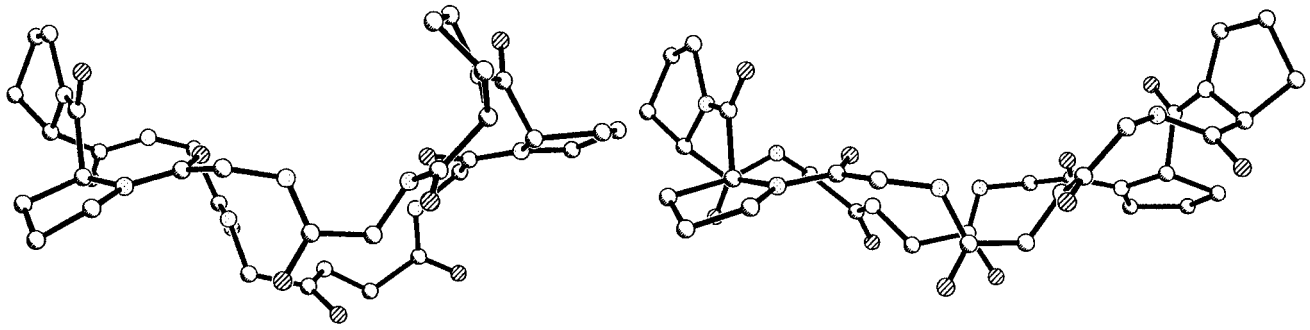

Figure 3. Cyclic peptide backbones for (left) phakellistatin 8 (**2**) and right antamanide (**1**).

theme among each of these three cyclic peptides (phakellistatin 8, stylopeptide 1 and antamanide), which contain residues occupying the left-handed α-helices region, is the presence of more than one proline residue, some of which are involved in turns in the cyclic backbone. Apparently the proline rings not only play a crucial role in the production of turns in the cyclopeptide ring, but a more subtle role in determining the orientation of some of the side chain substituents of the main cyclic backbone.

A closer examination of the solid-state conformations of both phakellistatin 8 and antamanide revealed an additional, rather intriguing feature involving the proline moieties and some of the aromatic side chains (e.g., Phe and Tyr moieties). The side chain substituents were seen to fold back over their

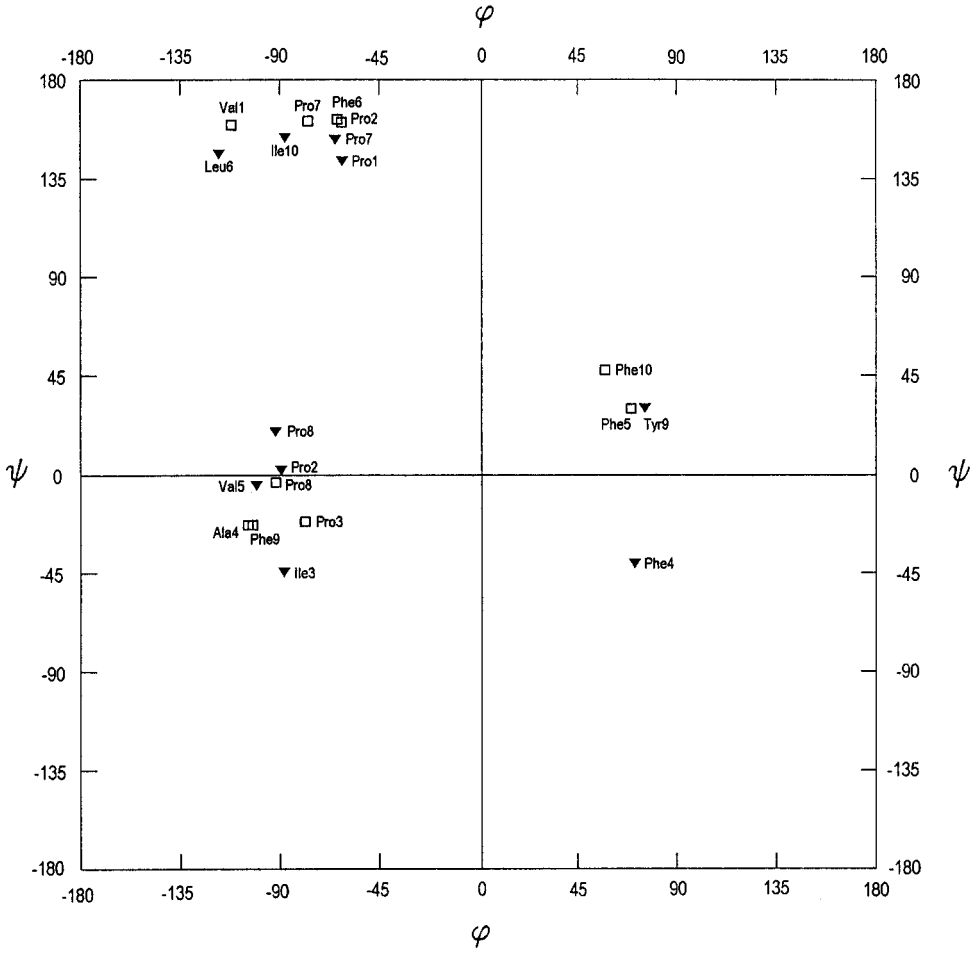

Figure 4. Ramachandran plot of crystal conformations for phakellistatin 8 (▼) and antamanide (□).

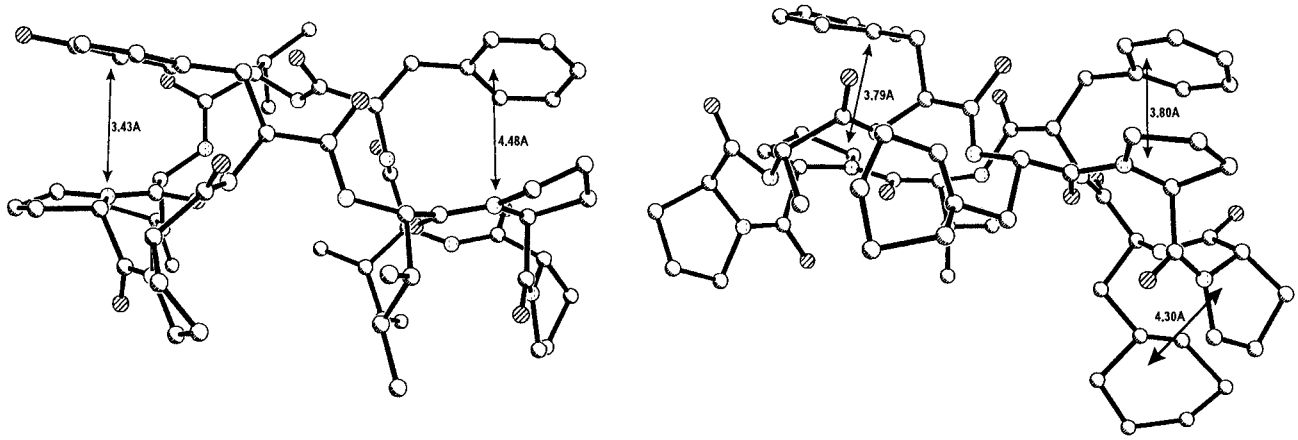

Figure 5. Aromatic ring coplanarity relationships between Pro rings and Tyr_9 and Phe_4 in phakellistatin 8 (**2**) (left) and between Pro rings and Phe_5, Phe_9 and Phe_{10} in antamanide (**1**) (right). Some side chain atoms (Ala_4 and Phe_6) in **1** have been excluded for clarity.

respective peptide backbones instead of extending outward into the, presumably, less sterically hindered regions perpendicular to the backbones. In addition, the side chains tended to assume an approximately coplanar orientation with respect to proline rings in each molecule. The coplanar relationship can be seen in Figure 5. With the Phe residues, a possible explanation for this aromatic ring-proline association may be due to the hydrophobic nature of the phenyl group. Because both the phakellistatin 8 and antamanide molecules are extensively hydrated in the solid state, projection of the hydrophobic Phe residues away from the peptide backbone into the surrounding hydrophilic solvent regions would be energetically less favorable then allowing the aromatic rings to project over the more hydrophobic regions afforded by the proline rings. With the Tyr aromatic ring, the hydrophobic, aromatic ring of this group also lies in a hydrophobic region proximate and coplanar to a proline ring, but the polar, phenolic hydroxyl end of Tyr projects into the surrounding solvent area where it is locked into position via hydrogen bonding with the water molecules, W-2 and W-5. Although preferential association and geometry relationships of certain types of amino acid side chains for one another (i.e., hydrophobic bonding and interactions) have been reported in the literature[32] and searched for systematically,[33] to our knowledge no reports of preferred association or geometry studies have been reported between aromatic residues, such as Phe and Tyr, and the proline ring. Perhaps the apparent association of the Phe and Tyr residues with the proline rings is purely coincidental or due to other, unknown factors. The nonbonded

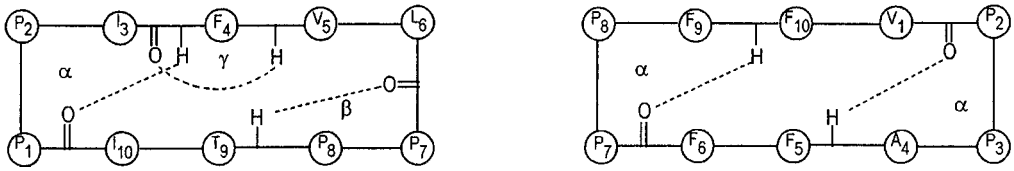

Figure 6. Schematic drawing of the intramolecular hydrogen bonds and reverse turns for phakellistatin 8 (**2**) (left) and antamanide (**1**) (right).

Table 5. Hydrogen Bonds for Phakellistatin 8

donor	acceptor	distance (esd), Å	angle,[a] deg	translation[b]
N4	O10′	2.90	163	000
N5	O3′	2.77	140	000
N9	O6′	2.84	138	000
N10	W-3	3.05	133	000
W-1	O2′	2.81	*c*	000
W-2	O9H	2.67	*c*	000
W-2	O9′	2.77	*c*	000[d]
W-3	O6′	2.94	*c*	000
W-4	O5′	2.74	*c*	000
W-4	W-2	2.68	*c*	000
W-5	O10′	2.99	*c*	000
W-6	O8′	2.78	*c*	000
W-6	W-4	2.44	*c*	$\bar{1}00$[d]
O-SO	W-1	2.82	*c*	00$\bar{0}$
O9H	W-5	3.25	*c*	00$\bar{1}$

[a] Angle at hydrogen. [b] Translations are along *x*, *y*, and *z*, respectively. [c] Hydrogen positions not determined. [d] Symmetry transformation, $^1/_2$+x, $^1/_2$-y, −z.

distances between the proline ring nitrogen atom and the closest associated aromatic ring atom range from 3.43 to 4.48Å for phakellistatin 8 and from 3.79 to 4.30Å for antamanide. These distances are near the outer limits (e.g., 3.75 Å) of what would be considered to be presumptive, shared contact distances (which are based upon van der Waal "dot surface" atomic radii) between noncovalently bonded atoms of amino acids.[33]

4.2. Hydrogen Bonding and Turn Types. All intra- and intermolecular hydrogen bonding interactions for phakellistatin 8 (**2**) are shown in Figure 1 and summarized in Table 5. As indicated previously, both the phakellistatin 8 and antamanide conformers are extensively hydrated in the solid state when crystallized from aqueous solvents. In the case of phakellistatin 8, inter- and intramolecular hydrogen bonding occurs between the peptide carbonyl oxygens O2′, O3′, O5′, O6′, O8′, O9′, and O10′ and amide hydrogens or water molecules. The inclusion of water molecules into the interior of the backbone ring is a unique feature exhibited by both of these peptide molecules. In the case of antamanide, the water molecules serve as transannular bridges between amide groups and provides a certain degree of rigidity to the cyclic backbone.[7i] Phakellistatin 8 also contains ring inclusion water molecules which are hydrogen bonded to the interior carbonyl oxygens of the Leu_6 (W-3···O6′, 2.94Å) and Ile_{10} (W-5···O10′) residues, but only the former serves a transannular bridge role. Any ring conformational rigidity in phakellistatin 8 is instead provided by three intramolecular amide hydrogen−carbonyl oxygen type hydrogen bonds which are involved in peptide turns. These intramolecular bonds can be characterized as follows: (1) a 5→1 transannular α-turn type H-bond, encompassing the Pro_1, Pro_2, and Ile_3 residues and involving the Phe_4 amide hydrogen and the Ile_{10} carbonyl (N4···O10′, 2.90 Å); (2) an intramolecular 3→1 type VIa γ-turn type of H-bond, encompassing the Phe_4 residue and involving the Val_5 amide hydrogen and the Ile_3 carbonyl (N5···O3′, 2.77 Å); and (3) an intramolecular 4→1 type VIa β-turn H-bond, encompassing the Pro_7 and Pro_8 residues and involving the Tyr_9 amide hydrogen and the Leu_6 carbonyl (N9···O6′, 2.84 Å). A schematic comparison of the intramolecular hydrogen bonds and reverse turns for phakellistatin 8 and antamanide is shown in Figure 6. In contrast to phakellistatin 8, both proline pairs of antamanide are involved in two, nearly symmetrical α-turns[8f] rather than participating in β-type turns. That the chain reversals for phakellistatin 8 and antamanide should be slightly different and that the latter should have symmetrical conformational aspects is to be expected. Antamanide possesses an approximate 2-fold rotation axis, relating peptide residues I with I+5, whereas phakellistatin 8 lacks such pseudo symmetry. It should be noted that a similar, two α-turn chain reversal conformation is also observed for the completely symmetrical [Phe_4,Val_6] antamanide analog, which has a true 2-fold rotation axis.[7e,f]

In addition to the extensive intermolecular H-bonding between water and the carbonyl oxygens of phakellistatin 8, nearly all of the water molecules are in turn bonded to other water molecules, to solvent atoms (the methanol hydroxyl) or to the Tyr_9 hydroxyl group. The involvement of the Tyr_9 hydroxyl function in H-bonding with W-2, resulting in a conformational locking of the tyrosine ring, has already been mentioned. Figure 1 shows this locking mechanism, which involves bridge formation between the two water molecules, W-2 and W-4, and spanning the Val_5 carbonyl oxygen O5′ and the Tyr_9 hydroxyl atom O9H. Direct interlinking of adjacent peptide molecules via H-bonding occurs with W-1 (O2′···W-1···O2′a) and W-2 (O9H···W-2···O9′a). The water molecule W-1 fulfills a unique role, in that it not only interlinks peptide molecules, but also the solvate molecule methanol. Since W-1 occupies a special position at $^1/_2$, $^1/_2$, *z*, as does the carbon atom of methanol (C-SO), both W-1 and methanol occur only once for each two phakellistatin 8 molecules in the crystalline matrix. More extended interlinking of peptide molecules via hydrogen bonding is also exhibited by the water molecules W-2, W-4, W-5, and W-6. Beyond the conformational locking bridge mentioned previously (O9H···W-2···W-4···O5′), an extended hydrogen-bonded bridge sequence involving W-2, W-4, and W-6 (O9′a···W-2···W-4···W-6···O8′a) occurs which serves to join three, symmetry-related phakellistatin 8 molecules in the crystalline matrix (see Figure 1). An additional bridge linking adjacent phakellistatin 8 molecules is also provided by W-5 (O9Ha···W-5···O10′).

4.3. Crystal Packing and Channel Formation. One of the more interesting features reported from the crystal structure studies of antamanide, as well as its symmetric [Phe_4,Val_6] isostructural analog, is the formation of large diameter continuous channels through the crystal lattices of these compounds.[7e−j] In the crystal structure of antamanide (**1**), the molecules are positioned in the cell such that a large continuous channel is formed in the *c* direction of the lattice with its center near $a = {}^3/_4$ and $b = {}^1/_2$, as depicted in Figure 7a. The channel is completely surrounded by hydophobic side chains of six Pro,

(32) (a) Kauzmann, W. In *Advances in Protein Chemistry*; Anfinsen, C., Anson, M., Bailey, K., Edsall, J. Eds.; Academic Press: New York, NY, 1959; Vol. 14, pp 37−47. (b) Némethy, G. *Angew. Chem., Intl. Ed. Engl.* **1967**, *6* (3), 195−280. (c) Hildebrand, J. *J. Phys. Chem.* **1968**, *72*, 1841−2. (d) Vinogradov, S.; Linnell, R. In *Hydrogen Bonding*; Van Nostrand Reinhold Co.: New York, NY, 1971; pp 223−56.

(33) Rowland, R.; Allen, F.; Carson, W.; Bugg, C. In *Crystallographic and Modeling Methods in Molecular Design*; Bugg, C., Ealick, S., Eds.; Springer-Verlag: New York, NY, 1990, p 234.

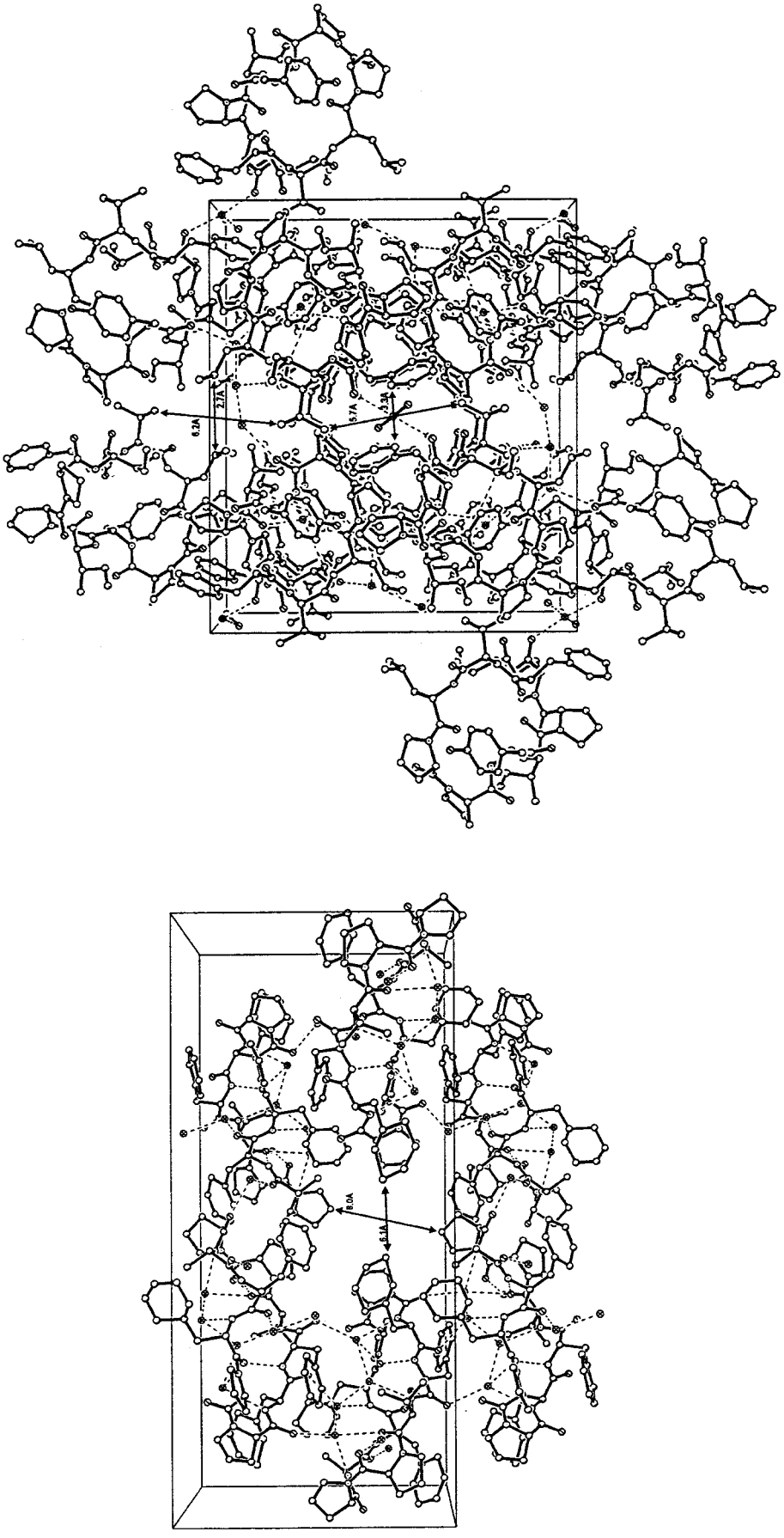

Figure 7. Cell packing diagrams showing channel formation in antamanide (a) and phakellistatin 8 (b). Water oxygen atoms are donated by ⊗ and hdyrogen bonding by dashed lines. The axial directions for both cells are *a*, ↓, *b* → and *c* out from page.

six Phe, and two Ala residues from adjacent molecules. The channel is quite large, with approximate dimensions of 6.1 Å in the *b* direction and 8 Å in the *a* direction. Because of the hydrophobic nature of the channel, only random molecules of crystallization solvent occupy the channel. In phakellistatin 8 (**2**), the molecules of the peptide are also stacked in such a manner as to provide two, parallel channels extending down the *c* axis (Figure 7b). The smaller of the two channels, centered at $a = 0.5$ and $b = 0.5$ in the unit cell, with approximate dimensions of 5.7 Å in the *a* direction and 3.3 Å in the *b* direction, is surrounded by the hydrophobic side chains of Phe, Pro, and Val residues. However, the channel does have some hydrophilic character, owing to the proximity of two carbonyl oxygens (O2′) from the Pro_2 residues of two independent peptide molecules of phakellistatin 8 extending into the channel. These oxygens are hydrogen bonded with one water molecule, W-1, which is located precisely in the center of the channel and positioned directly below (and thus obscured by) C-SO (the methyl substituent of a methanol solvent molecule), located in the exact center of the channel. This single molecule of methanol solvent is depicted as a linear, diagonal arrangement of three atoms in the center of Figure 7b. The end atoms represent the two $^1/_2$ occupancy hydroxyl atoms (O-SO) of methanol, and the central atom represents the methyl portion (C-SO) of methanol. Hydrogen bonding also occurs between W-1 and the two $^1/_2$ occupancy oxygen atoms, but this bonding is also obscured in Figure 7b by the C-SO...O-SO bonds. A second channel, with approximate dimensions of 2.7 Å by 6.2 Å, is positioned on the edges of the cell of phakellistatin 8 at the symmetry-related positions $a = 0.0$, $b = 0.5$, and $a = 0.5$, $b = 0.0$. The channel is very hydrophilic, being surrounded by the carbonyl oxygens O5′, O8′, and O9′, as well as the Tyr_9 hydroxyl atom O9H. As a result, the channel is extensively hydrated, being filled with the three water molecules W-2, W-4, and W-6, which form the water bridges between separate peptide molecules.

4.4. Proline Conformations. Because the pyrrolidine ring in the prolyl residue contains a planar nitrogen atom and four tetrahedral carbon atoms, the ring cannot be planar without inducing an inordinate amount of strain. Thus the ring can adopt a number of different, puckered conformations in which one or two of the ring carbon atoms are displaced above or below the plane defined by the nitrogen and the other atoms. To describe the various conformations adopted by the four prolyl residues in both phakellistatin 8 and antamanide, the method of Ashida and Kakudo[26e] has been used. By this method, the proline residues for phakellistatin 8 (2) can be classified as follows: Pro_1 C_s-C$^{\gamma}$*exo*, Pro_2 C_2-C$^{\beta}$*exo*(C$^{\gamma}$*endo*), Pro_7 C_s-C$^{\gamma}$*endo*, and Pro_8 C_2-C$^{\beta}$*exo*(C$^{\gamma}$*endo*). A similar analysis of antamanide (**1**) results in the following: Pro_2 C_s-C$^{\gamma}$*exo*, Pro_3 C_2-C$^{\beta}$*exo*(C$^{\gamma}$*endo*), Pro_7 C_s-C$^{\beta}$*exo*, and Pro_8 C_2-C$^{\beta}$*exo*(C$^{\gamma}$*endo*). Thus, the proline conformations for the first proline pairs, i.e., the Pro_1-Pro_2 sequence of phakellistatin 8 and the Pro_2-Pro_3 sequence of antamanide, are the same for both compounds. These identical proline conformations occur at the α-turn region of both molecules. The second proline pair sequence differs at Pro_7 for the two compounds, but the Pro_8 conformations are identical.

5. Concluding Remarks

The conformational properties of the cyclic decapeptide phakellistatin 8 (**2**) are remarkably similar to those of antamanide (**1**) and its structural isomers. The solid-state conformations of both of these peptides are unlike other, well-studied cyclic decapeptides such as gramicidin S and the tyrocidines, whose conformations have been shown to adopt a rigid, antiparallel *β*-pleated sheet type structure.[1a,2a,2c,30] Instead, both phakellistatin 8 and antamanide adopt a more flexible, extended "saddlelike" solid-state conformation, which is extensively hydrated when crystallized from aqueous solutions. Proline residues are intricately involved in the formation of this conformation, being situated at the head and tail of the saddle and producing the reverse turns observed in these cyclic peptides. In addition, in the solid state, both compounds exhibit channel formation and an apparent preferential association between the aromatic residues and the pyrrolidine residues.

Because of the very close structural relationships between phakellistatin 8 and phakellistatins 7 and 9, the question arises as to whether the latter two phakellistatins also have similar solid state conformations. Furthermore, do the phakellistatins form complexes with cations such as Na^+, Li^+, K^+, and Ca^{2+}, in a manner analogous to antamanide? If so, will the complexes be distorted into a cuplike conformation, as with antamanide? Do the phakellistatins have antidotal properties against the liver toxin phalloidin? If the latter is true, this fact would lend additional support to the theory that the toxin prophylactic activity of antamanide is indeed due to its ability to selectively complex Na^+ ions. That would suggest the peptide conformation allowing such complexation is of considerable significance. Thus, the possibility exists of using phakellistatin 8 (and possibly, phakellistatins 7 and 9) as biochemical probes in elucidating the antitoxin activity of antamanide. In addition, the ability (or failure) of the phakellistatins to form metal complexes (such as are implicated in the strong antineoplastic activity of the cyclic depsipeptide valinomycin) could provide further insight concerning the cancer cell growth inhibitory properties of phakellistatins 7−9. Such directions, as well as examination of the preferred solution conformation(s) for phakellistatin 8, will be pursued when we are able to prepare sufficient quantities of these cyclic decapeptides by total syntheses.

Acknowledgment. The essential financial support for this research was provided by Outstanding Investigator Grant CA44344-01-09 awarded by the Division of Cancer Treatment, Diagnosis and Centers, U. S. National Cancer Institute, DHHS, The Arizona Disease Control Research Commission and the Robert B. Dalton endowment fund. We thank Drs. Cherry Herald, Fiona Hogan, and Thomas Groy for their helpful discussions.

Supporting Information Available: Tables giving crystallographic and structure refinement data, atomic and hydrogen coordinates, isotropic and anisotropic displacement parameters, and bond lengths and angles for **2** and supplemental references (51 pages). See any current masthead page for ordering and Internet access instructions.

JA9626648